

Computer Vision-based Algae Removal Planner for Multi-robot Teams

Manoj Penmetcha^{†1}, Shaocheng Luo^{†1}, Arabinda Samantaray^{†1,2}, J. Eric Dietz³, Baijian Yang³
and Byung-Cheol Min¹

Abstract—Water pollution has caused increased incidence of algal growth around the globe. Harmful algae blooms result in massive economic losses. In this paper, a multi-robot based task planner is designed to remove excessive algae from water bodies and to identify algae build-up so that prompt action can be taken against its accumulation. Computer vision is incorporated to enable algae detection and area estimation based on training, comparing, and evaluating various advanced deep learning models using our custom algae dataset. We further propose a novel algorithm for robot resource allocation between bounding boxes of detected algae based on multi-variable optimization. This systematic solution is evaluated in a simulated environment, demonstrating how the robots are optimally assigned to the detected algae patches for algae removal.

Index Terms—Deep Learning, Computer Vision, Algae removal, Multi-robot systems, Resource allocation, Optimization

I. INTRODUCTION

Algae are primarily aquatic, uni- or multi-cellular organisms that contain chlorophyll [1]. In a healthy aquatic environment, algae are primary producers and therefore a critical foundation of the food chain. Algae also benefit humans by reducing the level of greenhouse gases in the atmosphere by fixing large quantities of CO_2 in the oceans [2], serving as a source of energy in the form of bio fuels, and acting as a cheap but highly effective means for wastewater treatment [3].

Under congenial ecological conditions, however, the rate of algae proliferation can increase exponentially, resulting in the formation of large algal colonies sometimes covering many square kilometers. Such colonies are known as harmful algal blooms (HABs). They have been found to be responsible for releasing paralytic, neurotoxic, diarrhetic, amnesic, and azaspiracid toxins, leading to the deaths of fishes, sea mammals, birds, and even humans [4].

Hence, it is extremely important that ponds, lakes, and rivers are constantly monitored and that prompt action is taken against any abnormal algae buildup. Currently, a highly promising solution to cleanup and monitoring of algae blooms is to use unmanned water surface vehicles (USVs)

[†] M. Penmetcha, S. Luo, and A. Samantaray contributed equally to this work (co-first authors).

¹ M. Penmetcha, S. Luo, and B.-C. Min are with the SMART Lab, Department of Computer and Information Technology, Purdue University, West Lafayette, IN 47907, USA. e-mails: {mpenmetc, luo191, minb}@purdue.edu

² A. Samantaray is now a Software Engineer at Cisco, San Jose, California. e-mail: samantarayarabinda@yahoo.com

³ B. Yang and J. E. Dietz are with the Department of Computer and Information Technology, Purdue University, West Lafayette, IN 47907, USA. e-mails: {byang, jedietz}@purdue.edu}

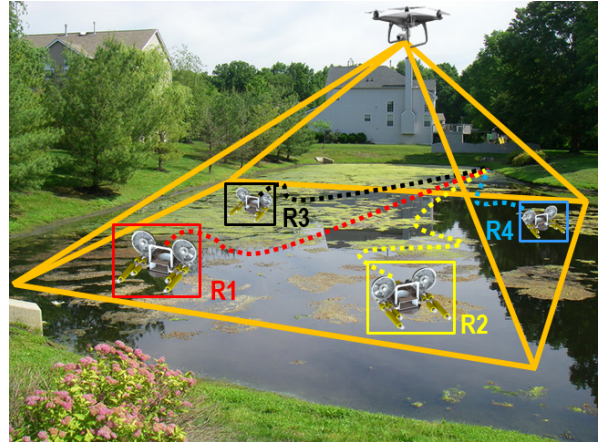


Fig. 1. Demonstration of image capture of an algae patch using a drone. Our proposed system detects algae using deep learning. The system also allocates robots to detected bounding boxes to remove the algae.

[5] and underwater vehicles [6] equipped with sensors and removal end-effectors. Unmanned aerial vehicles (UAVs) can be used to monitor algae blooms and provide a global map for USV distribution [5].

As a concrete solution to task planning for algae removal using multi-robot teams, this paper contributes to the research community in the following ways:

- We introduce a computer vision-based algae removal planner for use with multi-robot teams.
- We develop a computer vision algorithm based on deep learning that can accurately detect and locate algae in water bodies, irrespective of variation in camera parameters, environmental conditions, orientation of the captured image, or the presence of significant background clutter in the form of vegetation, buildings, etc.
- We introduce a resource allocation algorithm that uses the proposed computer vision algorithm in a multi-robot environment.

This paper is organized as follows: In Section II, we describe current algae monitoring systems and their shortcomings. Section III presents our proposed solution for algae detection and removal using deep learning. In Section IV, we evaluate system performance and analyze the results obtained, followed by presentation of the conclusion and future works in Section V.

II. RELATED WORK

The coupling of human-caused effects such as eutrophication by agricultural runoff, dumping of untreated industrial

and household effluents, and transportation of foreign algae species in ballast water with natural phenomena such as storms, tsunamis, currents [7], and global warming has been cited as the root cause for the rising incidence of HABs in water bodies around the globe. This rising incidence has increased the relevance of effective algae monitoring methodologies in the modern world.

Algae monitoring techniques can be roughly classified into three categories: *in-situ* sampling, computer vision-based techniques, and hyperspectral remote sensing using satellite or aircraft.

A. *In-situ* Sampling

In-situ sampling is effected through performing on-site sampling and then transporting those samples to laboratories for further evaluation. Although on-site sampling is done at regular intervals, this methodology is extremely time- and labor-intensive. Also, the possibility of contaminated samples negatively affecting observations is high [8].

B. Computer Vision based Techniques

Computer vision-based algae monitoring systems have been developed that exploit the distinctive green or greenish-blue color characteristic of algae. However, such traditional computer vision pipelines do not have high repeatability; they depend significantly on the effectiveness of their feature detectors or their segmentation procedures. These can be rendered ineffective by environmental conditions such as fluctuating illumination, occlusion, or the presence of comparable objects in the background.

The algae monitoring system in study [9] uses a combination of color-based segmentation, species-specific features, and an underwater camera; this implies that it cannot be applied on a different hardware platform such as an UAV, USV, or smartphone, and also that it is susceptible to occlusion and variations in illumination, which are regular occurrences in an outdoor environment. Similarly, the novel approach presented in the paper [10], which combines the use of a smartphone camera and the inertial sensors present on a robotic fish to detect the shoreline and subsequently perform image segmentation to detect algal blooms, is optimized for their specific hardware platform (i.e. robotic fish) and is susceptible to variable illumination, occlusion, and shadows cast by surrounding vegetation.

Similar limitations can also be observed in the work of [11], which made use of a local binary pattern texture detector to detect algae. However, the authors only utilized a UAV platform and have not described their systems performance in the event of using images taken from different orientations or higher elevations. Also, considering that their detector is only trained on iconic images of algae, grass and water, they have not presented any results describing the impact of comparable objects such as trees, plants, and seaweeds present in image backgrounds on their algae monitoring system.

Similarly, the authors of [12] only considered images taken from the ground and did not describe the speed with which

their vision system could detect algae. Hence, it is difficult to ascertain whether this method could be employed on mobile platforms such as UAVs, USVs, and airplanes, which operate in different environments.

C. Satellite Remote Sensing

Satellite-based remote sensing for algae monitoring makes use of the increase in diffused reflectance caused by the presence of algal pigment in a body of water [13]. Spectral data is used as input for detection methods such as reflectance classification algorithms, reflectance band-ratio algorithms and spectral band difference algorithms [14]. However, although the aforementioned algorithms are successful at monitoring algal blooms in the open ocean, they have been ineffective when applied to coastal water and bodies of water with significant human activity because the presence of organic material and suspended particles distorts the reflectance spectrum. Also, issues such as unavailability of real-time data, irregular site revisit times, low resolution of publicly-available satellite products such as LANDSAT or MODIS (> 30m), and exorbitant costs of proprietary systems such as QuickBird [15] make the use of satellite imagery difficult for a general-purpose algae monitoring system.

Hence, an economically feasible algae detection and removal planner that can be used on a wide variety of platforms (e.g. UAVs, USVs, airplanes, and even smartphones) would significantly facilitate administrators and civilians in removing algae blooms and monitoring water bodies. The development of such a system is the major contribution of this paper. To strengthen the utility of this system, we consider a multi-robot application scenario in which we use global images of the workspace taken from UAVs and detect algae patches in the water using an object detection model. Multi-robots in the water body are assigned to these algae patches by the proposed resource allocation algorithm. After reaching the algae patches, the robots can perform appropriate actions based on their capabilities. Fig. 1 presents an overview of the system we propose in this paper.

III. WORK-FLOW OF THE PROPOSED TASK PLANNER

The proposed algae removal task planner mainly consists of two layers: the *Algae Detection Layer* and the *Multi-robot Planner Layer*. The system workflow we developed is depicted in Fig. 2, with individual steps described in the following subsections.

A. *Algae Detection Layer*

1) *Dataset and Labelling*: For the purpose of this research, we collected a dataset of images taken from ground and aerial vehicles depicting algae in pools, lakes, ponds, etc. The distribution of images across training and testing sets is shown in Table I. These images were collected with a variety of resources, and priority was given to generating a diverse dataset. We collected some of the images ourselves, obtained some from online resources, and generated some through artificial simulations. We utilized the Tensorflow Object Detection API to train our chosen models to detect algae

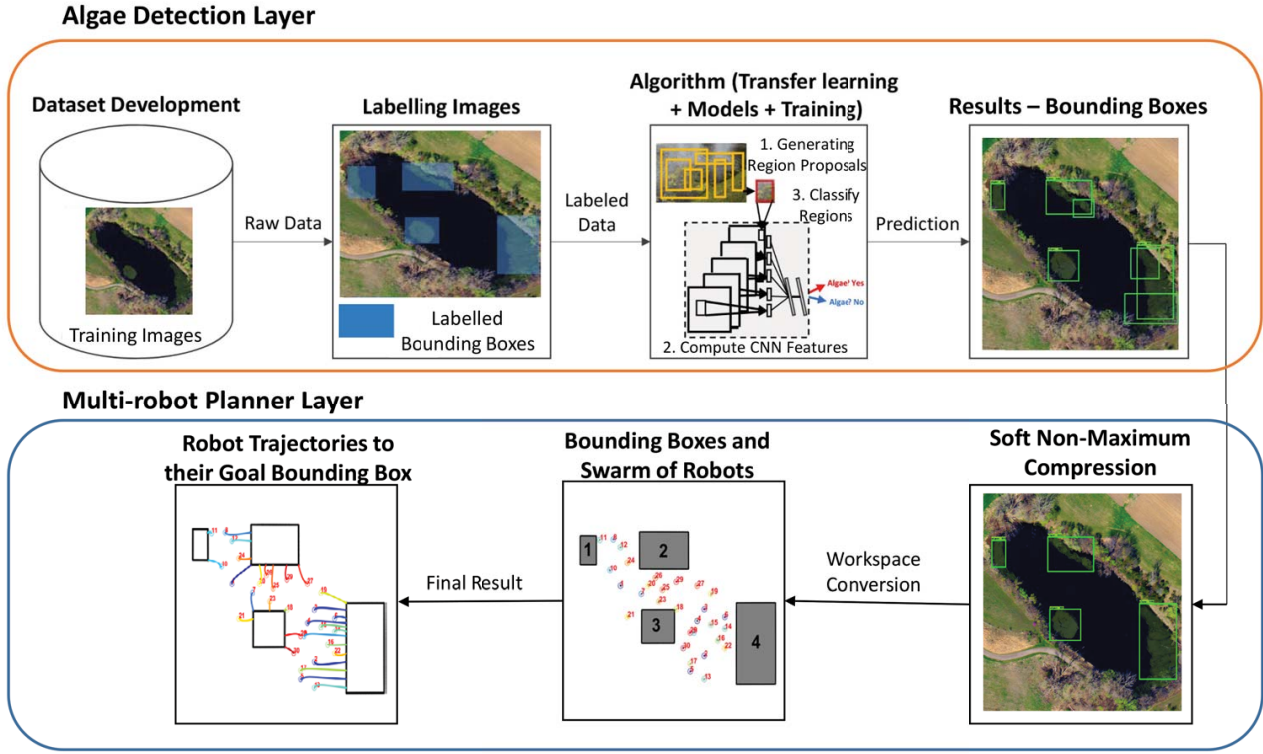


Fig. 2. Workflow of the proposed algae removal planner. Its components can broadly be categorized into the *Algae Detection Layer* and the *Multi-robot Planner Layer*.

[16]. The Tensorflow Object Detection API is an open source framework based on the tensorflow library that provides a well-structured environment for developing, training, testing, and deploying deep learning models.

2) *Deep Learning Algorithms:* An algae monitoring system that conceivably could be used from mobile platforms such as USVs, UAVs, airplanes, etc. has to detect and locate algae at near real-time speeds with high accuracy. Models using Faster R-CNN [17], Single Shot Detector (SSD) [17], and Region-based Fully Convolutional Networks (R-FCN) [17] have shown near real-time object detection on conventional datasets such as COCO and PASCAL-VOC with very high accuracy, making them applicable to our envisaged scenario. To mitigate the effects of a small training dataset and to replicate external environmental conditions such as variable illumination, fluctuating contrast, and blurring, we augmented our dataset by applying transformations such as randomly changing the brightness, contrast, hue, color, and saturation. To customize the pre-trained networks for our dataset, we applied a decaying learning rate of 10% every

5000 steps, and we changed the final layers to reflect that our dataset contains only one class of objects.

3) *Results-Bounding Boxes:* After training the model, the neural network populates a result array with coordinates, scores, and classes, which can be found in Fig. 3(a), and number of detections for each frame/image, as shown in Fig. 3(b). We convert the coordinates from this array into appropriate bounding boxes by applying the following equation:

$$Coordinate_k = Box_i^j \cdot ImageWidth \quad (1)$$

where $Coordinate_k$ denotes the current coordinate, $k \in \{\text{left, right, top, bottom}\}$, i denotes the index of Box , $j \in \{0, 1, 2, 3\}$, and $ImageWidth$ is the image width. Subsequently, these image coordinates can then be used to visualize the predicted bounding boxes, as shown in Fig. 3(b).

B. Multi-robot Planner Layer

To develop a multi-robot planner, we propose a resource allocation algorithm that assigns robots to detected patches for the removal of algae.

1) *Non-maximum Suppression:* One issue that we observed in the object detection results is that the algorithms R-CNN and R-FCN produced multiple detections on the same algae patch. This is a consequence of the underlying workings of neural networks. However, in order to apply our proposed resource allocation algorithm, an algae patch must be detected singly. To achieve this, we employed a soft non-maximum suppression (NMS) algorithm [18]. NMS makes

TABLE I

DISTRIBUTION OF IMAGES ACROSS TRAINING, VALIDATION, AND TEST SETS (D.= DETECTION)

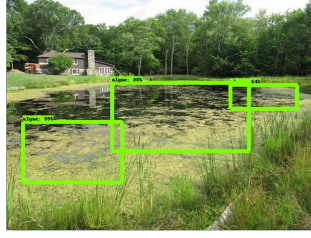
	Training	Validation	Testing (D.)
Ground Images	277	79	41
Aerial Images	150	43	20

```

[(b'algae', 0.99449414, array
([0.534338, 0.05314522, 0.79369253, 0.37
690017], dtype=float32)),
(b'algae', 0.99377173, array
([0.36726111, 0.34154907, 0.66079456,
0.78759915], dtype=float32)),
(b'algae', 0.64734805, array
([0.37421644, 0.72547305, 0.47608191,
0.94418544], dtype = float32))]

```

(a) Results



(b) Resultant Image

Fig. 3. Representative results generated by the model and their visualization on the associated image.

use of scores on each bounding box to remove overlapping bounding boxes. The results of using this algorithm are shown in Fig. 4.

2) *Resource Allocation Algorithm*: Provided M number of bounding boxes $\mathcal{B}_i, i \in \{1, \dots, M\}$, with their areas denoted as $A_i, i \in \{1, \dots, M\}$, multi-robots can be optimally allocated among these bounding boxes as resources for algae cleaning. As an infrastructure of multi-robot allocation, wirelessly networked robot teams have shown significant improvement and demonstrated strong capability in tasks that are similar to our scenario, such as rendezvous control for surveillance [19], [20], collaborative coverage for spill cleaning [21], urban search and rescue [22], and unknown environment exploration [23].

The robot resource allocation should meet the following three goals:

- (i) The allocation should guarantee that at least one robot is assigned to each bounding box, assuming that the number of robots N is greater than the number of bounding boxes M ;
- (ii) The total distance traveled by the assigned robots is minimized; and
- (iii) The number of robots assigned to a given bounding box is proportional to its area.

The first goal guarantees that no bounding box will be neglected. The second goal is to minimize the energy consumption of robots while maneuvering to their assigned bounding box. The third goal can help in balancing the workload across all operational robots, because a larger bounding box may require more effort (e.g. algae volume being collected, total length of traveled path, etc). As the individual robots have identical coverage capabilities, deploying a uniform density of robots to each Box makes the completion time deterministic.

This paper formulates the proposed resource allocation problem into a binary integer linear programming (ILP) problem as below in (2)-(6). The solution was obtained using a generic ILP solver in MATLAB. Optimization yields a globally optimal and deterministic solution for the objective function, which is suitable for the proposed resource allocation problem.



(a) Without NMS

(b) With NMS

Fig. 4. Illustration of the removal of multiple bounding boxes from single objects by NMS.

$$\min \sum_{j=1}^M \sum_{i=1}^N z_{ij} \cdot \|d_{ij}\| \quad (2)$$

subject to

$$\sum_{i=1}^N z_{ij} \geq 1, \quad \forall j \in \{1, 2, \dots, M\}. \quad (3)$$

$$\sum_{j=1}^M \left(\frac{A_j}{\sum_{i=1}^N z_{ij}} - \rho \right)^2 \leq \gamma^2 \rho^2 \quad (4)$$

$$\sum_{j=1}^M z_{ij} = 1, \quad \forall i \in \{1, 2, \dots, N\} \quad (5)$$

$$z_{ij} = \begin{cases} 1, & \text{if robot } R_i \text{ is allocated to } \mathcal{B}_j, \\ 0, & \text{otherwise,} \end{cases} \quad (6)$$

$$\forall i \in \{1, 2, \dots, N\}, \forall j \in \{1, 2, \dots, M\}$$

The objective function (2) seeks to minimize the total traveling displacement of every robot while maneuvering to its designated bounding box, in keeping with the second proposed goal. In (2), $\|d_{ij}\|$ denotes the linear distance from robot R_i to one of the four bounding boxes \mathcal{B}_j , while the binary variable vector z_{ij} is defined in (5). Constraint (3) represents the first proposed goal and guarantees each bounding box is attended to by at least one robot. Constraint (4) is to satisfy the third proposed goal, and allocating a number of robots proportional to the area of the bounding box. Here, ρ is the ideal average density of robots in bounding boxes, i.e. $\rho = \frac{N}{\sum_{i=1}^M A_i}$, while a coefficient γ is introduced to restrain the variance of this density among different bounding boxes. Constraint (5) means that any given robot can be allocated to only one bounding box, while the last constraint (6) shows the binary characteristic applied on optimization variables z_{ij} .

3) *Robot Path Planning*: A robot can move from its current position to its goal position by applying the artificial potential field (APF) method, for instance in [21]. Provided

TABLE II
 MODEL PERFORMANCE: ACCURACY OF CLASSIFICATION (ACCURACY, PRECISION, AND RECALL), ACCURACY OF DETECTION (VALIDATION MAP AND TEST MAP), AND SPEED OF THE DETECTION (FPS (GPU) AND FPS (CPU)) (VALID. = VALIDATION)

	Accuracy	Precision	Recall	Valid. mAP	Test mAP	FPS (GPU)	FPS (CPU)
Faster R-CNN	72%	74.00%	71.15%	38.68%	23.46%	2.83	0.62
R-FCN	82%	78.33%	90.38%	38.14%	21.44%	2.72	0.58
SSD	50%	52.08%	48.07%	23.72%	17.29%	19.37	5.16

that the robots follow the same single integrator model as in [21], the control law for each robot is is given as:

$$U(\mathbf{q}_i) = \frac{1}{2}\xi d(\mathbf{q}_i, \mathbf{q}_i^g)^2, \quad (7)$$

where \mathbf{q}_i denotes a robot current position, \mathbf{q}_i^g denotes its goal position on the boundary of the designated bounding box, and ξ is a scaling parameter. The input in velocity \mathbf{u} for the robot is therefore the gratitude of (7), i.e.

$$\mathbf{u} = -\nabla U(\mathbf{q}_i) = \xi(\mathbf{q}_i^g - \mathbf{q}_i). \quad (8)$$

IV. EVALUATION AND RESULTS

A. Algae Detection Models

In this section, we will describe the results obtained from three different neural networks using different criteria.

1) *Parameters and Hardware Used for Evaluation:* Since our objective was to develop a computer vision system that can rapidly detect and locate algae in water bodies, we focused on the following three evaluation metrics:

- Precision and recall – to evaluate the accuracy of our system in detecting whether a given water body contains algae or not;
- Mean average precision (mAP) – to evaluate how accurately our system can locate an algal bloom in a water body;
- Speed to evaluate the speed at which each neural network detects algae, so as to validate the appropriateness of this approach for use in mobile platforms such as USVs, UAVs, airplanes, etc.

To evaluate the object detection models, we used a HP Pavilion laptop that had an Intel(R) Core(TM) i7-6500U CPU and an NVIDIA GeForce 940MX GPU.

2) *Algae Detection Results:* A reliable algae monitoring system should have high *recall* (if algae is present, then the system should detect it) and high *precision* (if the presence of algae is predicted, then algae should in fact be present). To evaluate the competence of our system in detecting algae, we performed a binary classification between two sets of images, one having water bodies containing algae and the other having water bodies not containing algae. Trained versions of each model were tested on the aforementioned images, and their results are given in Table II (see column 2–4). Since there were only two classes of images, SSD performed very poorly; its ability to detect algae was akin to that of random selection, which implies that it is not at all suitable for algae

detection. Meanwhile, Faster R-CNN and R-FCN had nearly similar *Precision* values, but the high *Recall* value of R-FCN indicates that it is highly robust and nearly always detects an algae bloom if one is actually present.

Accurate algae localization from an image would enable us to generate precise world coordinates corresponding to where the algae blooms are present. To evaluate the detection accuracy of the three trained models, we used mean average precision (mAP); these values are presented in Table II (see column 5 and 6). All three models showed reasonably acceptable accuracy with regard to algae bloom localization. Notably, both Faster R-CNN and R-FCN have higher detection accuracy than SSD on both the test and validation datasets. Also, mAP values are lower for the test dataset than the validation dataset. We believe this resulted from the fact that we had chosen the most complex images for the test dataset, ones containing significant amounts of background clutter (trees, buildings, roads, etc).

The speed with which each model detected algae in an input image is also shown in Table II (see the last two columns). In contrast to results observed for classification and detection accuracy, SSD outperforms the other two models in terms of detection speed when using either a CPU or GPU. Of the three models used here, SSD has the lowest computational cost [24]. However, seeing as algal blooms grow in static or slow-moving water bodies, the detection speeds obtained for all three models are satisfactory for use in an algal monitoring system, particularly when implemented on a GPU.

Despite using state-of-art object detection models, we observed a few occasions in which either algae was not detected or the surrounding vegetation was labeled as algae, which could be a topic for further study and refinement. Some examples are presented in Fig. 5. The most likely cause for such incidences is that the only defining characteristic of



Fig. 5. Representative images showing incorrect or missed detections of algae.

algae is its green color; this is also the most common color found in an outdoor environment. A larger training dataset that enables the neural network to learn more intricate features would be able to detect algae with greater consistency.

We acknowledge that our dataset is small and requires improvement. We plan to expand the dataset and make it public when it is ready for broader use. Through the work described in this paper, we were able to identify the direction that we need to take to make a robust algae detection model.

B. Resource Allocation Implementation

To exemplify the resource allocation and validate the effectiveness of the optimization method, we simulated pictures of a lake with algae detected and bounded in $M = \{2, 3, \text{ and } 4\}$ bounding boxes (Fig. 6) and performed optimization on the cost function of (2). The optimization results and the process of robots being driven to the corresponding bounding boxes were visualized using Robotarium, a $3m \times 3m$ scaled-down multi-robot testbed [25], which is shown in the last column of Fig. 6. As illustrated in Fig. 6, $N = \{10, 20, \text{ and } 30\}$ robots were involved in the operation, with their starting positions randomly distributed throughout the workspace. The number of robots allocated to each bounding box based on the optimization are listed in Table III. From the results, we see that the number of robots allocated for a bounding box was in proportion to the area of the box. Meanwhile, compromising with the previous goal, each robot moved in a shortest distance to its associate box. The allocation results demonstrate a consistency in terms of different numbers of bounding boxes and locations.

For all three scenarios, the trajectories by which all robots maneuvered to their respective goal positions are depicted in the last column of Fig. 6 for all the three scenarios. More details can be found in the paper video:

<https://youtu.be/bBPMFwSzHz0>.

V. CONCLUSION AND FUTURE WORK

In this work, we develop a deep learning-based algae detector and a multi-robot system-based algae removal planner. The planner is based on an optimization algorithm and achieves an optimal resource allocation. For the detection of algae, we compared state-of-the-art object detectors Faster R-CNN, R-FCN, and SSD. Our final conclusion is that an algae monitoring system based on the R-FCN model

would be highly robust, accurate, and rapid, thereby enabling effective recognition of algae in real time. We anticipate that these findings will help us develop a more robust algae detection model. We further demonstrated the efficacy of the proposed resource allocation optimization method and virtually verified its capability in diverse environments and with different settings. Our future works will focus on improving performance through developing a larger dataset and implementing field tests. Moreover, we will use this task planner to facilitate the development of a multi-robot ecosystem composed of autonomous UAVs and USVs; this ecosystem would be responsible for monitoring water bodies and removing HABs in real environments.

REFERENCES

- [1] "General algae information," <http://www.ecy.wa.gov/programs/wq/plants/algae/lakes/AlgaeInformation.html>, accessed: 2017-09-30.
- [2] "Ocean's living carbon pumps: When viruses attack giant algal blooms, global carbon cycles are affected," <https://www.sciencedaily.com/releases/2014/10/141021101510.htm>, accessed: 2017-10-12.
- [3] H. Fallowfield and M. Garrett, "The treatment of wastes by algal culture," *Journal of Applied Microbiology*, vol. 59, no. s14, 1985.
- [4] T. Okaichi, *Sustainable Development in the Seto Inland Sea, Japan*. Terra Scientific Publishing Company, 1997.
- [5] S. Jung, H. Cho, D. Kim, K. Kim, J.-I. Han, and H. Myung, "Development of algal bloom removal system using unmanned aerial vehicle and surface vehicle," *IEEE Access*, vol. 5, pp. 22 166–22 176, 2017.
- [6] F. Zhang, O. Ennasr, E. Litchman, and X. Tan, "Autonomous sampling of water columns using gliding robotic fish: Algorithms and harmful-algae-sampling experiments," *IEEE Systems Journal*, vol. 10, no. 3, pp. 1271–1281, 2015.
- [7] K. G. Sellner, G. J. Doucette, and G. J. Kirkpatrick, "Harmful algal blooms: causes, impacts and detection," *Journal of Industrial Microbiology and Biotechnology*, vol. 30, no. 7, pp. 383–406, 2003.
- [8] H. B. Glasgow, J. M. Burkholder, R. E. Reed, A. J. Lewitus, and J. E. Kleinman, "Real-time remote monitoring of water quality: a review of current applications, and advancements in sensor, telemetry, and computing technologies," *Journal of Experimental Marine Biology and Ecology*, vol. 300, no. 1-2, pp. 409–448, 2004.
- [9] C. S. Tan, P. Y. Lau, S.-M. Phang, and T. J. Low, "A framework for the automatic identification of algae (neomeris vanbosseae ma howe): U 3 s," in *Computer and Information Sciences (ICCOINS), 2014 International Conference on*. IEEE, 2014, pp. 1–6.
- [10] Y. Wang, R. Tan, G. Xing, J. Wang, X. Tan, and X. Liu, "Energy-efficient aquatic environment monitoring using smartphone-based robots," *ACM Transactions on Sensor Networks*, vol. 12, no. 3, 2016.
- [11] S. Jung, D. Kim, K. Kim, and H. Myung, "Image-based algal blooms detection using local binary pattern," 2016.
- [12] A. C. Kumar and S. M. Bhandarkar, "A deep learning paradigm for detection of harmful algal blooms," in *Applications of Computer Vision (WACV), 2017 IEEE Winter Conference on*. IEEE, 2017, pp. 743–751.
- [13] G. A. Carvalho, P. J. Minnett, L. E. Fleming, V. F. Banzon, and W. Baringer, "Satellite remote sensing of harmful algal blooms: A new multi-algorithm method for detecting the florida red tide (karenia brevis)," *Harmful algae*, vol. 9, no. 5, pp. 440–448, 2010.
- [14] D. Blondeau-Patissier, J. F. Gower, A. G. Dekker, S. R. Phinn, and V. E. Brando, "A review of ocean color remote sensing methods and statistical techniques for the detection, mapping and analysis of phytoplankton blooms in coastal and open oceans," *Progress in oceanography*, vol. 123, pp. 123–144, 2014.
- [15] K. F. Flynn and S. C. Chapra, "Remote sensing of submerged aquatic vegetation in a shallow non-turbid river using an unmanned aerial vehicle," *Remote Sensing*, vol. 6, no. 12, pp. 12 815–12 836, 2014.
- [16] M. Abadi, A. Agarwal, P. Barham, E. Brevdo, Z. Chen, C. Citro, G. S. Corrado, A. Davis, J. Dean, M. Devin, *et al.*, "Tensorflow: Large-scale machine learning on heterogeneous distributed systems," *arXiv preprint arXiv:1603.04467*, 2016.
- [17] Z. Zhao, P. Zheng, S. Xu, and X. Wu, "Object detection with deep learning: A review," *CoRR*, vol. abs/1807.05511, 2018. [Online]. Available: <http://arxiv.org/abs/1807.05511>

TABLE III

NUMBER OF ROBOTS ALLOCATED PER BOUNDING BOX UNDER THREE DIFFERENT SCENARIOS

Scenario 1 (N=10)	Bounding boxes (2)	\mathcal{B}_1	\mathcal{B}_2	-	-
	Areas (m^2)	0.541	0.478	N/A	N/A
Allocated robots (#)	5	5	N/A	N/A	
Scenario 2 (N=20)	Bounding boxes (3)	\mathcal{B}_1	\mathcal{B}_2	\mathcal{B}_3	-
	Areas (m^2)	0.475	0.508	0.327	N/A
	Allocated robots (#)	8	7	5	N/A
Scenario 3 (N=30)	Bounding boxes (4)	\mathcal{B}_1	\mathcal{B}_2	\mathcal{B}_3	\mathcal{B}_4
	Areas (m^2)	0.079	0.325	0.193	0.572
	Allocated robots (#)	2	9	6	13

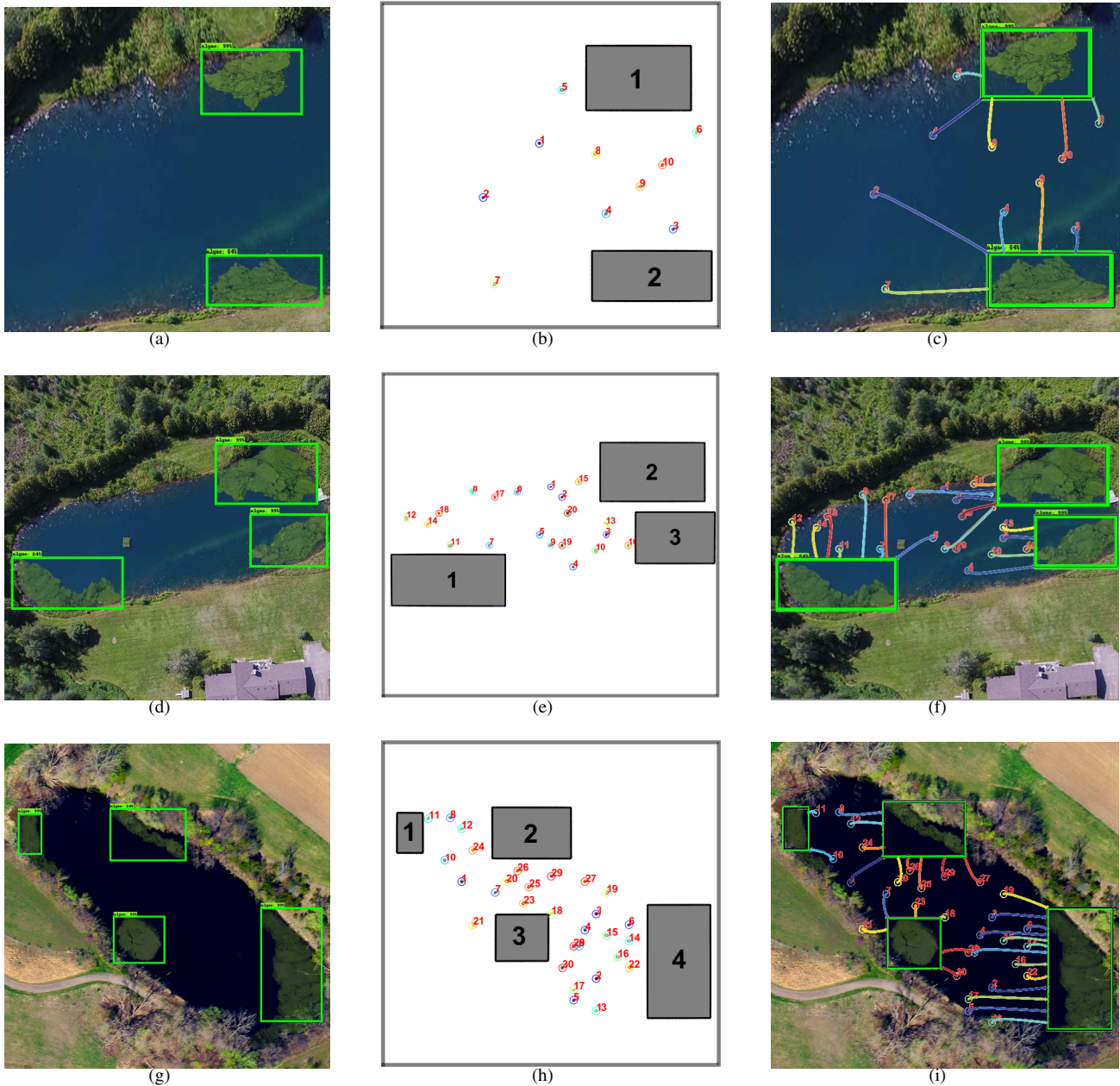


Fig. 6. (a), (d), and (g) are the ground truth of workspace that contains algae patches, labeled with *Scenario 1, 2, and 3* with the number of bounding boxes being $M = 2, 3,$ and 4 . (b), (e), and (h) show the initial robot distributions in the workspace. (c), (f), and (i) indicate the trajectories of the deployed robots during allocation for the three scenarios, respectively.

[18] N. Bodla, B. Singh, R. Chellappa, and L. S. Davis, "Improving object detection with one line of code," *CoRR*, vol. abs/1704.04503, 2017. [Online]. Available: <https://arxiv.org/abs/1704.04503>

[19] R. Parasuraman, J. Kim, S. Luo, and B.-C. Min, "Multipoint rendezvous in multirobot systems," *IEEE transactions on cybernetics*, 2018.

[20] S. Luo, J. Kim, R. Parasuraman, J. H. Bae, E. T. Matson, and B.-C. Min, "Multi-robot rendezvous based on bearing-aided hierarchical tracking of network topology," *Ad Hoc Networks*, vol. 86, pp. 131–143, 2019.

[21] S. Luo, J. H. Bae, and B.-C. Min, "Pivot-based collective coverage control with a multi-robot team," in *2018 IEEE International Conference on Robotics and Biomimetics (ROBIO)*. IEEE, 2018, pp. 2367–2372.

[22] M. Erdelj, M. Król, and E. Natalizio, "Wireless sensor networks and multi-uav systems for natural disaster management," *Computer Networks*, vol. 124, pp. 72–86, 2017.

[23] B.-C. Min, E. T. Matson, and J.-W. Jung, "Active antenna tracking system with directional antennas for enhancing wireless communication capabilities of a networked robotic system," *Journal of Field Robotics*, vol. 33, no. 3, pp. 391–406, 2016.

[24] L. T. Nguyen-Meidine, E. Granger, M. Kiran, and L. Blais-Morin, "A comparison of cnn-based face and head detectors for real-time video surveillance applications," in *2017 Seventh International Conference on Image Processing Theory, Tools and Applications (IPTA)*, Nov 2017, pp. 1–7.

[25] D. Pickem, P. Glotfelter, L. Wang, M. Mote, A. Ames, E. Feron, and M. Egerstedt, "The robotarium: A remotely accessible swarm robotics research testbed," in *2017 IEEE International Conference on Robotics and Automation (ICRA)*. IEEE, 2017, pp. 1699–1706.